

Nuclear multifragmentation of ^{32}S and ^{28}Si in emulsion nuclei

M El-Nadi[†], M S El-Nagdy[‡], A Abdelsalam[†], E A Shaat[†], N Ali-Mossa[§],
Z abou-Moussa[†], Kh Abdel-Waged[¶], W Osman[†] and F A Abdel-Wahed[‡]

[†] Physics Department, Faculty of Science, Cairo University, Cairo, Egypt

[‡] Physics Department, Faculty of Science, Helwan University, Ain Helwan, Cairo, Egypt

[§] Basic Science Department, Faculty of Engineering, Zagazig University, Benha Branch, Egypt

[¶] Physics Department, Faculty of Science, Benha University, Egypt

Received 27 May 1998, in final form 26 August 1998

Abstract. The fragmentation of ^{32}S (3.7 A GeV) and ^{28}Si (14.6 A GeV) is investigated as a function of the degree of disintegration of different components of photoemulsion nuclei. The experimental measurements show nearly energy-independent behaviour throughout the studied charge, size and multiplicity distributions of fragments produced from the two projectile beams. The various stages of the interactions, from the initial impact through to the final formation of clusters, are theoretically treated as follows. (i) The first stage of the interaction is modelled by the Glauber approach, using Reggeon parametrization for the nucleon–nucleon scattering amplitude. (ii) The additional inelastic interaction of secondary particles, produced in the primary stage, with other nucleons of the nucleus is analysed in the framework of a Reggeon-theory inspired model. (iii) The phenomenological percolation–evaporation model is used to describe the spectator part of the nucleus.

1. Introduction

Recently, considerable interest [1–4] has centred around the idea of nuclear multifragmentation (MF) (fragmentation of highly excited nuclei into many fragments with charge $Z \geq 2$).

A theoretical description of nuclear MF generally starts from the assumption of two stages, phases of the interaction. In the first stage, the incident nucleons scatter on the target ones, ejecting some of them and leaving a certain amount of energy to the spectator part, which forms rather excited residues. In the second stage, after escape of the participant nucleons, the residues decay through evaporation of neutrons and light nuclei (p, d, ^3He and ^4He) for low excitation energy. At higher excitation energies, the residues disintegrate into fragments of intermediate mass (IMF).

The models of quantum molecular dynamics (QMD) [5] or models of intranuclear cascade (e.g. FRITIOF [6], VENUS [7], DPM [8] . . .) are used to examine the first stage of the process. Unfortunately, most of them cannot simultaneously be applied at 3.7 A GeV and 14.6 A GeV. To understand the second stage, statistical models [9, 10] are frequently applied.

In combination with the statistical nuclear MF model, the model of relativistic quantum molecular dynamics (RQMD) has begun to be used in recent times [11] to study the nuclear MF.

¶ Author for correspondence. E-mail address: KHELWAGD@FRCU.EUN.EG

In this study, we are interested in analysing events produced from interactions of ^{32}S (3.7 A GeV) and ^{28}Si (14.6 A GeV) with the different components of emulsion nuclei. The details of the interactions at initial impact are studied by the Glauber approach, using the Reggeon parametrization for the nucleon–nucleon (NN) scattering amplitude. The secondary interaction processes are treated using a simple Regge model of nuclear disintegration [12–15].

The Glauber–Regge model (briefly discussed in section 3) enables one to estimate the nuclear residual masses and charges. Using the relation between the residual mass and excitation energy proposed in [13, 14] we reach a complete description of the ensemble of nuclear residual masses, charges and excitation energy. The effect of the fragmentation of the spectator part of the nucleus is evaluated using the phenomenological percolation–evaporation model. The combination between the Glauber–Regge model and the percolation–evaporation models will be referred as the combined model.

The multiplicity distributions of non-interacting charges (the Q value) of ^{32}S (3.7 A GeV) and ^{28}Si (14.6 A GeV) interactions with different target nuclei are compared with the Glauber–Regge model calculations in section 4. Also in this section, the charge distribution of all projectile fragments (PFs) (having charge $Z \geq 2$) as well as the multiplicity distribution of these PFs are compared with the predictions of the combined model. Finally our consideration ends with a brief summary in section 5.

2. Experimental procedures

This work was carried out using the nuclear emulsion technique which is very suitable for studying nucleus–nucleus (AA) interactions because it registers all charged particles of individual event in a 4π -geometry due to its high spatial resolution.

For this paper, two stacks were used. The first was of type BR—two emulsion pellicles of dimensions $10 \times 20 \text{ cm}^2$ and thickness $600 \mu\text{m}$ which were horizontally exposed to ^{32}S ions at 3.7 A GeV in the Dubna Synchrotron. The second stack was of FUJI-type whose pellicles have dimensions $10 \times 16 \text{ cm}^2$ and thickness $600 \mu\text{m}$. These pellicles were horizontally exposed to ^{28}Si ions at 14.6 A GeV at Brookhaven National Laboratory (BNL) Alternating Gradient Synchrotron (AGS).

Both kinds of emulsion are sensitive to singly charged relativistic particles such that the grain density of these ionization tracks is about 30 per $100 \mu\text{m}$ at minimum ionization. All fragmentation products, irrespective of charge and velocity, are detectable. The pellicles of each stack were doubly scanned (fast in the forward and slow in the backward direction) using the along the track method such that each track was followed until it either interacted or left the pellicle. Through a total scanned length of 75.0 and 121.8 m, 785 and 962 inelastic interactions were detected for the studied ^{32}S and ^{28}Si projectiles, respectively, giving respective mean free paths $\lambda_{\text{exp}} = 9.6 \pm 0.3 \text{ cm}$ [16] and $12.7 \pm 0.4 \text{ cm}$. The corresponding experimental cross sections ($\sigma_{\text{exp}} = 1/\lambda_{\text{exp}}N$, where N is the total number of target nuclei per unit volume) are $\sigma_{\text{exp}} = 1314 \pm 47 \text{ mb}$ [16] and $1000 \pm 40 \text{ mb}$, respectively. The values of λ_{exp} and σ_{exp} for ^{28}Si (14.6 A GeV) are close to that given for a similar experiment [17] ($\lambda_{\text{exp}} = 12.4 \pm 0.4 \text{ cm}$ and $\sigma_{\text{exp}} = 1023 \pm 34 \text{ mb}$).

In each event, the charges $Z \geq 2$ of individual PFs were determined by the combination of several methods which include grain, gap, and δ -ray densities [18]. More details on the charge determination of PFs are given in [19]. PFs essentially travel with the same speed as that of the parent beam nucleus, so the energy of the produced PFs is high enough to distinguish them easily from the target fragments.

Beside PF's tracks, the target-associated slow-moving track particles emitted from

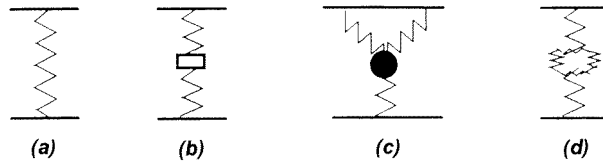


Figure 1. The diagrams representing NN interactions (heavy lines) through Reggeon exchange (zigzag lines): (a) non-enhanced type (soft); (b) hard scattering type; (c) triple Reggeon diagram (the full circle corresponds to a Reggeon vertex); (d) loop Reggeon diagram.

an excited emulsion target are also considered in this paper. These track particles are known as black prongs, N_b , having velocity $v < 0.2c$ with residual range $R < 3$ mm, corresponding to kinetic energy $E_k < 20$ MeV; and grey ones, N_g (recoil protons) with velocity $0.2c < v < 0.7c$ and $R \geq 3$ mm correspond to $20 \leq E_k \leq 375$ MeV. The multiplicity of heavy tracks N_h , is generally defined as $N_h = N_g + N_b$.

All PFs are emitted in a very forward direction within an angle given by the Fermi momentum. The fragmentation cone is defined by a critical angle. The values of these critical angles are found to be equal 3° and 13 mrad for 3.7 and 14.5 A GeV, respectively. The quantity Q per event which measures the total charge of non-interacting projectile nucleons is also calculated.

3. Model prescriptions

3.1. Primary interactions

The AA interaction is usually described using the optical approximation of the multiple scattering model (Glauber theory). The calculation of Glauber AA cross sections and the impact parameter distributions require evaluation of the NN scattering amplitude. An energy independent Gaussian parametrization of the NN scattering amplitude is frequently applied. A different approach based on Reggeon parametrization of the NN amplitude is suggested in [20]. Since in the present work we use two projectiles having different energies, we will apply the latter parametrization in the case of AA interactions. The NN scattering amplitude corresponding to the diagrams of the type shown in figure 1 is

$$\gamma_i(b, s) = \frac{\sigma_i}{8\pi a_i} e^{-b^2/4a_i}. \quad (1)$$

Here (i) stands for the soft (so), hard (h), triple (tp) and loop (l) Reggeon exchange mechanisms. s is the total energy squared in the CMS. As in [20], we use $a_h = a$, $a_{so} = a_{tp} = a_l = a + \alpha' \ln(s \text{ GeV}^{-2})$ and $a = 3.52 \text{ GeV}^2$, $\alpha' = 0.24 \text{ GeV}^{-2}$ for the slope parameters in the scattering amplitude of (1). At 3.7 A GeV the values of σ_i are taken as $\sigma_s = 44.29$ mb, $\sigma_h = 0.00$ mb, $\sigma_{tp} = -9.76$ mb and $\sigma_l = 10.53$ mb. The corresponding values at 14.6 A GeV are $\sigma_s = 46.38$ mb, $\sigma_h = 0.00$ mb, $\sigma_{tp} = -7.55$ mb and $\sigma_l = 5.48$ mb. Therefore, at the present energy the triple and loop diagrams may cancel each other and the dominant diagram contribution to the primary interactions is the one that corresponds to soft interactions (figure 1(a)).

Using the standard assumptions of the multiple scattering model and treating the NN amplitude as the sum of amplitudes due to multi-Reggeon exchange:

$$\gamma(b, s) = \gamma_{so}(b, s) + \gamma_h(b, s) - \gamma_{tp}(b, s) - \gamma_l(b, s) \quad (2)$$

we obtain the inelastic scattering amplitude of nucleus A on nucleus B in the form of a sum of contributions of graphs of the type shown in figure 1:

$$F_{A,B}(s, \mathbf{q}) = \frac{i p_A}{2\pi} \int d^2 b e^{i \mathbf{q} \cdot \mathbf{b}} \langle \psi_A, \psi_B | 1 - \prod_{j=1}^A \prod_{k=1}^B (1 - \gamma(\mathbf{b} - \mathbf{r}_j + \boldsymbol{\tau}_k, s)) | \psi_B, \psi_A \rangle \quad (3)$$

where p_A is the momentum of the projectile nucleus A , \mathbf{q} is the transferred transversal momentum, \mathbf{b} is an impact parameter, $\{\mathbf{r}_j\}$, $j = 1, 2, \dots, A$ and $\{\boldsymbol{\tau}_k\}$, $k = 1, 2, \dots, B$ are the respective coordinates of nucleons within nucleus A and nucleus B on the impact parameter plane (these coordinates are measured from the centre of mass of each nucleus). $\psi_{A,B}$ are the wavefunctions of both nuclei.

From (3) it is possible to find the production cross section (corresponding to the production of new particles) (see [21, 22]):

$$\begin{aligned} \sigma_{AB}^{\text{prod}} = & \int d^2 b \left\{ 1 - \prod_{i=1}^A \prod_{k=1}^B (1 - p(\mathbf{b} - \mathbf{r}_i + \boldsymbol{\tau}_k, s)) \right\} \cdot |\psi_A(\mathbf{r}_1, \dots, \mathbf{r}_A)|^2 \\ & \times \prod_{i=1}^A d^3 r_i |\psi_B(\mathbf{t}_1, \dots, \mathbf{t}_B)|^2 \prod_{i=1}^B d^3 t_i \end{aligned} \quad (4)$$

$$p(\mathbf{b}, s) = \gamma(\mathbf{b}, s) + \gamma^*(\mathbf{b}, s) - \gamma(\mathbf{b}, s)\gamma^*(\mathbf{b}, s).$$

Equation (4) may be rewritten in some form where each of its terms would be interpreted as a probability of some process

$$\begin{aligned} \sigma_{AB}^{\text{prod}} = & \int d^2 b \left\{ \prod_{i=1}^A \prod_{j=1}^B \frac{p(\mathbf{b} - \mathbf{r}_i + \boldsymbol{\tau}_j, s)}{1 - p(\mathbf{b} - \mathbf{r}_i + \boldsymbol{\tau}_j, s)} \cdot \prod_{k=1}^A \prod_{l=1}^B (1 - p(\mathbf{b} - \mathbf{r}_k + \boldsymbol{\tau}_l, s)) \cdot \right. \\ & + \frac{1}{2} \cdot \prod_{\substack{i=1, j=1 \\ i \neq j}}^A \prod_{k=1}^B \frac{p(\mathbf{b} - \mathbf{r}_i + \boldsymbol{\tau}_k, s)}{1 - p(\mathbf{b} - \mathbf{r}_i + \boldsymbol{\tau}_k, s)} \cdot \frac{p(\mathbf{b} - \mathbf{r}_j + \boldsymbol{\tau}_k, s)}{1 - p(\mathbf{b} - \mathbf{r}_j + \boldsymbol{\tau}_k, s)} \\ & \left. \times \prod_{l=1}^A \prod_{m=1}^B (1 - p(\mathbf{b} - \mathbf{r}_l + \boldsymbol{\tau}_m, s)) + \dots \right\} \cdot \\ & |\psi_A(\mathbf{r}_1, \dots, \mathbf{r}_A)|^2 \prod_{i=1}^A d^3 r_i |\psi_B(\mathbf{t}_1, \dots, \mathbf{t}_B)|^2 \prod_{i=1}^B d^3 t_i. \end{aligned} \quad (5)$$

Here the first term in the first braces is interpreted as the probability that the only one inelastic collision between i th nucleon from nucleus A and j th nucleon from nucleus B takes place through Reggeon exchange. The second term describes the probability of inelastic collision of the k th nucleon from nucleus B with i th and j th nucleons in A nucleus, etc.

Therefore, sampling of NN scattering amplitude (3) over the impact parameter (\mathbf{b}) yields the exclusive multi-Reggeon contributions which are needed for the construction of inelastic events in the primary stage of the interaction.

3.2. Secondary interactions

When using the above discussed model to describe AA interactions it is necessary to supplement it with a mechanism for including cascading in the spectator parts of the nucleus [12, 14].

The model [12] suggests that in the course of a hadron–nucleus (hA) collision, each of the interactions of the incident hadron with nucleons of a target nucleus initiates a cascade of

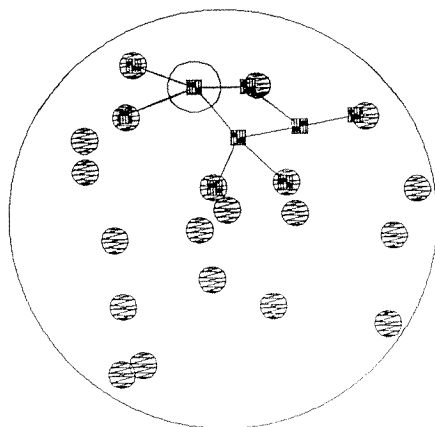


Figure 2. Reggeon ‘cascade’ in hA scattering in the impact parameter plane. The position of the projectile hadron is marked by an open circle, the positions of nuclear nucleons by closed circles, reggeon exchanges by straight lines and the square points are the coordinates of the Reggeon interaction vertices.

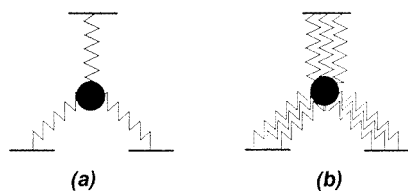


Figure 3. (a) An enhanced diagram which represents the interaction of a projectile nucleon with two target nucleons through Reggeon splitting. (b) An enhanced diagram representing the interaction with several Reggeons. The symbols are as in figure 1.

Reggeon exchanges (see figure 2). The Regge exchange amplitudes are taken in the ordinary Gaussian form. The dependence on the nucleon longitudinal coordinates is disregarded as in the Glauber approximation. It is assumed that all the nucleons involved in the Regge cascade leave the nucleus.

The calculation of amplitudes and cross sections for cascade interactions requires a consideration of enhanced diagrams i.e. diagrams with an interaction between Reggeons. It has been shown that the interference of enhanced diagrams in the central region is destructive (see also equation (2)). In the fragmentation regions, the yield of enhanced diagrams leads to the enrichment of the spectrum by slow particles.

As in [23, 24], we assumed that the Reggeon interaction vertices are small. Therefore, of the full set of enhanced diagrams, the only important ones will be those containing vertices where one of the Reggeons splits into several, which in turn interact with different nucleons of the nucleus (figure 3(a)). In studying interactions with nuclei, however, it is convenient in the spirit of the Glauber approach, to deal not with individual Reggeons, but with sets of them interacting with a given nucleon of the nucleus (figure 3(b)). Unfortunately, the Reggeon method of calculating the sum of the yields of enhanced diagrams in the case of hA and AA interactions is not developed for practical tasks. Taking the complexity of the problem into account, we invoked from [12] the simplest phenomenological approach that allows for generation of the exchange Reggeon diagrams.

The yield of the enhanced diagram of figure 3(b) is given by

$$Y_c = G \int_{\epsilon}^{Y-\epsilon} d\xi' d^2b' F_{N\pi}(\mathbf{b} - \mathbf{b}', Y - \xi') F_{\pi N}(\mathbf{b}' - \mathbf{s}_1, \xi') F_{\pi N}(\mathbf{b}' - \mathbf{s}_2, \xi') \quad (6)$$

where G is the three reggeon vertex constant, $Y = \ln s$ is the rapidity of the projectile hadron, ϵ is the cutoff parameter, $F_{\pi N}$ is the amplitude of πN elastic scattering, \mathbf{b} is the impact parameter of incident hadron, \mathbf{s}_1 and \mathbf{s}_2 are impact coordinates of two nuclear nucleons, and \mathbf{b}' , ξ' are coordinates of reggeon splitting vertices in the impact parameter rapidity space. Using Gaussian parametrization for $F_{\pi N}$ ($F_{\pi N} = \exp(-|\mathbf{b}|^2/R_{\pi N}^2)$) and neglecting its dependence on energy, we obtain,

$$Y_c \simeq G(Y - 2\epsilon) \frac{R_{\pi N}^2}{3} \exp(-(\mathbf{b} - (\mathbf{s}_1 + \mathbf{s}_2)/2)^2/3R_{\pi N}^2) \times \exp(-(\mathbf{s}_1 - \mathbf{s}_2)^2/2R_{\pi N}^2) \quad (7)$$

where $R_{\pi N}$ is the radius of the πN interaction. (Formula (7), assumes that the nuclear size is much greater than the range of hadron–nucleon interactions.) As seen from (7), Y_c is independent of the longitudinal coordinates and the multiplicity of the produced particles; that is cascading occurs in the impact parameter plane, and not in the three-dimensional space of the nucleus. Schematically, the process can be represented as in figure 2.

At large \mathbf{b} , the first exponent of (7) can be considered (in a crude approximation) as an effective amplitude of the interaction of the projectile hadron with the first nuclear nucleon. In this case the second exponent on the right-hand side of expression (7) has to be treated as the probability of involving the second nucleon in the interaction. Bearing in mind the weak dependence of the AA interaction characteristics on the form of the NN elastic scattering amplitude, we neglect the difference between the NN amplitude and the effective one. In line with these considerations, an algorithm of the Monte Carlo simulation of the cascade processes was formulated [12] as follows.

(1) Nucleon coordinates of colliding nuclei were sampled according to the Saxon–Wood distribution for nuclei with $A \geq 12$ while for lighter nuclei we used a Gaussian distribution. We also took into account the conservation of the nuclear centre-of-mass motion.

(2) The impact parameter was chosen according to [21].

(3) At a given impact parameter and given coordinates of the nuclear nucleons (in the corresponding reference frames), the interacting or ‘wounded’ nucleons of the nuclei were identified as above.

(4) One has to look for all the spectator nucleons of the residual nucleus. If the i th spectator nucleon is at the impact parameter distance $b_{ij} = |\mathbf{s}_i - \mathbf{s}_j|$ from the j th ‘wounded’ nucleon, then it is considered to be involved in the process with a probability

$$W = C_{nd} \exp\left(-\frac{b_{ij}^2}{r_c^2}\right). \quad (8)$$

where $r_c = 1$ fm is the mean interaction radius and $C_{nd} = 0.35$ is a strength factor. If $C = 0$, the whole cascade process reduces to the pure Glauber case, i.e. no cascading.

(5) If the number of newly involved nucleons is not equal to zero, one has to repeat step (2). At this point one only needs to consider the newly involved nucleons. If the number of the newly involved nucleons otherwise equals zero, then the procedure must be stopped.

It should be noted that the values of C_{nd} and r_c are previously determined [12] from data [25] on proton interactions with light (C, N and O) and heavy (Ag and Br) components of photoemulsion at 3.6 A GeV. We will not change the values of these parameters in order to check the sensitivity of the present results to them.

The procedure outlined above allows one to determine the number of spectator nucleons (A_{res}) as well as the sum of all charges (Z_{res}). These quantities are identified as the mass number and charge of the residual nucleus.

3.3. Nuclear fragmentation

When using the Glauber–Regge model to describe fragmentation induced by ^{28}Si or ^{32}S nuclei, it is necessary to combine it with a mechanism for including fragmentation of the spectator part of the projectile nucleus. There are two competing regimes for the latter process: either slow evaporation or fast multifragmentation of the spectator part of the residual nucleus.

We have adopted an assumption which unites the evaporation and statistical approaches to nuclear fragmentation [26]. It is assumed that the spectators cannot support an excitation energy higher than ϵ_{max} without breaking. At every collision, the spectators either decay by evaporation of the residues if the excitation energy is lower than ϵ_{max} or break into many fragments if it is larger.

In modelling evaporation, (in the case of excitation energy below ϵ_{max}), the standard evaporation model is used [27].

The fragmentation process is modelled in the percolation approach [28]. Here the relative location of the spectator nucleons is assumed to obey Maxwell–Boltzmann distribution i.e. $W(P_r) = \frac{1}{(2\pi\mu kT)^{3/2}} e^{-P_r^2/2\mu kT}$, where P_r is the relative momentum between any two nucleons, μ is the reduced mass and, finally, T is the temperature of the system. Therefore, the probability of breaking the bonds between any two nucleons can be written as

$$p = \frac{4\pi}{(2\pi\mu kT)^{3/2}} \int_{\sqrt{2\mu B}}^{\infty} e^{-P_r^2/2\mu kT} P_r^2 d^2 P_r \quad (9)$$

where B is the binding energy (taken as 8 MeV) and $T = 2/3E_{\text{ex}}$, with E_{ex} being the excitation energy. A cluster is identified if the nucleons are connected directly or indirectly by bonds.

The excitation energy of the spectator part of the nucleus was estimated in [26, 29, 30] for hA interactions as the sum of contributions for inelastic and elastic interactions of nucleons in the nucleus, and is distributed as

$$F(E_{\text{ex}}) = \frac{1}{\bar{E}} \exp\left(\frac{-E_{\text{ex}}}{\bar{E}}\right) \quad (10)$$

where \bar{E} is the average energy per NN collision.

To apply this approach to AA interactions we assumed [13, 14] that each spectator nucleon placing at a distance less than or equal to 2 fm from a nucleon touched at the first stage of the interaction receives an energy distributed according to (10). The sum of the energies transferred to the spectator nucleons gives the excitation energy. Unlike [26, 29, 30], this method will obviously lead to zero excitation energy when all the spectator nucleons are ejected.

The boundary between the spectator part of the nucleus and the involved parts at the first stage of the interaction, which determines the excitation energy, depends on the size of the colliding nuclei and also on the impact parameter. For instance, in AA interactions, the excitation energy rises with decreasing impact parameter from $R_A + R_B$ to 0 approaching a maximum and then falls (where $R_{A(B)}$ is the radius of nucleus $(A(B))$), where according to [26, 29, 30] it must gradually increase.

Table 1. The percentage of total projectile disintegration with varied degree of target break-up. The calculations (in parentheses) are based on equation (4).

Projectile	^{28}Si	^{28}Si	^{32}S	^{32}S
Energy (GeV)	3.7 A (GeV)	14.6 A (GeV)	3.7 A (GeV)	200 A (GeV)
$N_h = 0, 1$	8.36 ± 1.00 (9.70)	12.00 ± 1.40 (9.89)	3.99 ± 1.13 (10.28)	16.89 ± 2.58 (10.76)
$N_h = 2-7$	29.54 ± 2.07 (30.39)	28.35 ± 2.10 (30.42)	27.3 ± 3.26 (30.74)	27.02 ± 3.40 (30.82)
$N_h \geq 8$	62.1 ± 3.35 (59.88)	59.24 ± 2.74 (59.68)	68.71 ± 5.96 (58.97)	56.08 ± 5.44 (58.41)
Reference	[1]	present work	present work ^a	[1]

^a These results were previously published in [31].

The most recent results [3] obtained from the analysis of Au on Au and Cu at 600 A MeV show that the experimentally determined excitation energies are close to the mean binding energy of nuclei (between 8 and 10 MeV). As in [13, 14] we fix the value of \bar{E} at 10 MeV.

The mean excitation energy that corresponds to the evaporation process is calculated in [26] as a function of the bombarding energy for various targets and projectiles. It is shown that the mean excitation energy (ϵ_{\max}) reaches the limiting value of about 3 MeV independently of the target and of the projectile, when the incident energy is above 2 A GeV. Following [26], the value of ϵ_{\max} is kept at 3 MeV.

The calculation of residuals followed by the percolation procedures allows the global simulation to be made for ^{32}S and ^{28}Si interactions at 3.7 A GeV and 14.6 A GeV. In the subsequent discussion we will refer to this approach as the combined model.

4. Results and discussions

Table 1 shows the experimental fraction of events with total projectile disintegration (TD) given by this work for ^{28}Si (14.6 A GeV) and ^{32}S (3.7 A GeV) and that obtained by EMU01 collaboration [1] for ^{28}Si (3.7 A GeV) and ^{32}S (200 A GeV) after being normalized. This table also gives a comparison between the experimental and calculations which are based on equation (4). The TD events are defined as those events where only projectile fragments with charge $Z \leq 2$ remain. Such events are obtained at three different ranges of N_h . These groups are: (a) $N_h = 0, 1$, where the events are mainly quasinucleon ones i.e. those resulting from the interactions with H nucleus or with only one bound nucleon in either a CNO or AgBr nucleus, (b) $2 \leq N_h \leq 7$, in which the interactions are mostly due to collisions with CNO in addition to some peripheral collisions with AgBr and (c) $N_h \geq 8$ representing collisions with AgBr nuclei with a substantial degree of disintegration. It is seen (except for 3.7 A GeV ^{32}S interactions with $N_h = 0, 1$) that within the margin of errors, there is an agreement between the fraction for each range of N_h in TD events and the corresponding calculations.

Figure 4 illustrates the multiplicity distributions of Q values of the non-interacting part of the projectile nucleus (i.e. $Q = \sum_i n_i Z_i$, where n_i is the number of PFs with $Z \geq 1$ in an event) for 14.6 A GeV ^{28}Si and 3.7 A GeV ^{32}S at the three mentioned ranges of N_h . The full and broken curves represent the calculations according to the Glauber-Regge model

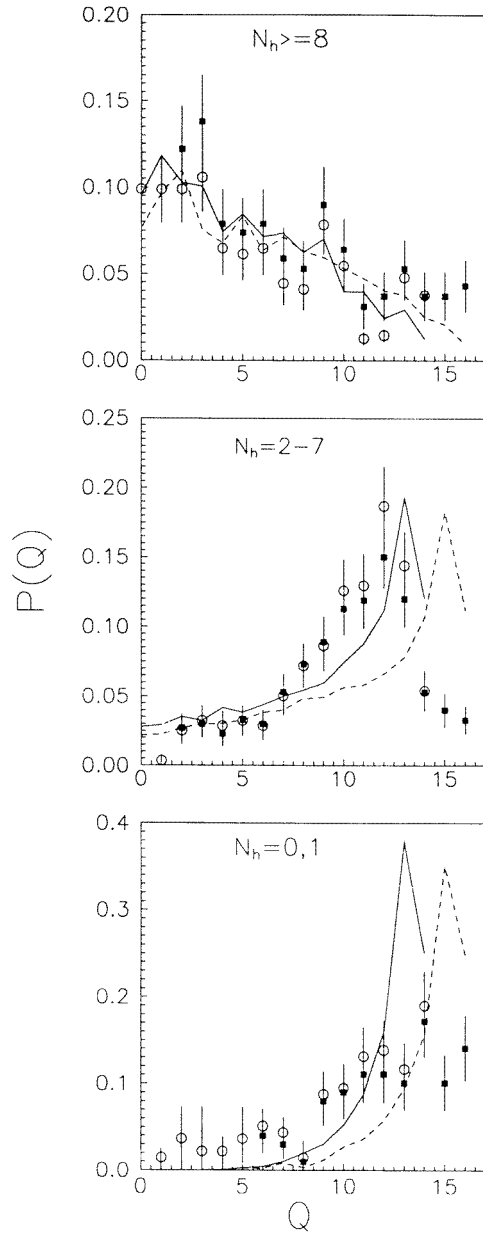


Figure 4. The Q distributions of ^{28}Si (14.6 A GeV) and ^{32}S (3.7 A GeV) interactions: bottom, with a quasinucleon type ($N_h = 0, 1$); middle, with the CNO type ($2 \leq N_h \leq 7$) and top, with AgBr type ($N_h \geq 8$). The points correspond to the data (see the legends on the figures). The full (broken) line is the calculations for ^{28}Si (^{32}S) interactions respectively, according to the Glauber–Regge model.

for ^{28}Si and ^{32}S , respectively. Experimental and predicted distributions are normalized to unity. It is interesting to note that for central and near-central events ($N_h \geq 8$), there is a good agreement between the experimental data and the calculations for both beams. In the case of $2 \leq N_h \leq 7$, the points are qualitatively described by the model where an agreement can only be seen for small values of Q . As for the events with $N_h = 0, 1$, the experimental results and the model follow the same trend. However, the model deviates from the data in the most peripheral interactions (larger Q values) due to the possible presence of electromagnetic events.

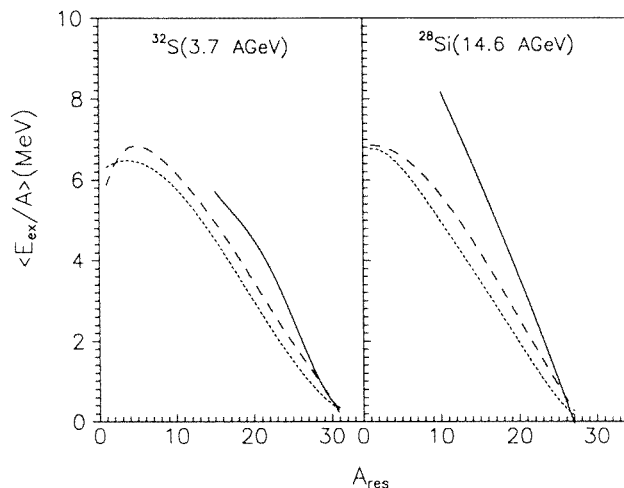


Figure 5. Results of the Glauber-Regge calculations. Mean specific excitation energy ($\langle E_{ex}/A \rangle$) as a function of the mass number A_{res} of the primary spectator of ^{32}S (3.7 A GeV) (left) and ^{28}Si (14.6 A GeV) (right) interactions: full curve, with a quasinucleon type ($N_h = 0, 1$); broken curve, with the CNO type ($2 \leq N_h \leq 7$); and dotted curve, with AgBr type ($N_h \geq 8$).

Figure 4 also indicates that for $N_h \geq 8$ events, the major contribution is toward the small values of Q characterizing the violent processes in these central and near central events. On the other hand, for quasinucleon events ($N_h = 0, 1$), the major contribution is toward the large values of Q characterizing the gentle processes. Regardless the results for $Q \geq 14$, the same observation applies for the CNO and peripheral AgBr events ($2 \leq N_h \leq 7$). The observations of low probability for the large values of Q ($Q \geq 14$) maybe due to the contamination of some collisions with AgBr in the region $2 \leq N_h \leq 7$.

A quantitative knowledge of the energy transfer to the primary spectator is indispensable for any interpretation of the multifragment decay. The mean excitation energy ($\langle E_{ex}/A \rangle$) as a function of the mass A_{res} of the projectile spectator is studied in figure 5 with the Glauber-Regge model. The energy deposits in the spectator system are obtained using (10). From the figure one notices that:

- the slopes of $\langle E_{ex}/A \rangle$ versus A_{res} grow steeper with decreasing mass of the target and energy of the projectile;
- the maximum of the specific energy that can be reached with a given target depends strongly on the target mass and less on the energy of the projectile.

Figure 5 would also permit checks against other cascade-type models for the initial stage and could provide the input for tests of other fragmentation models.

The experimental charge distribution of PFS having charge $Z \geq 2$ for 14.6 A GeV ^{28}Si and 3.7 A GeV ^{32}S , are obtained at the three different ranges of N_h . These charge distributions are shown in figure 6. The full and broken curves represent the corresponding calculations using the combined model for ^{28}Si and ^{32}S , respectively. Both the experimental charge distribution and the calculations are normalized to unity.

From this figure one can see that the charge distributions are nearly independent of the beam energy. The experimental data are qualitatively described by the predictions of the combined model. Quantitatively, it is seen that for large Z values, the charge distributions decrease, remain level and increase for $N_h \geq 8$, $2 \leq N_h \leq 7$ and $N_h = 0, 1$, respectively. This reflects the effect of the target size on the fragmentation of the projectile, especially

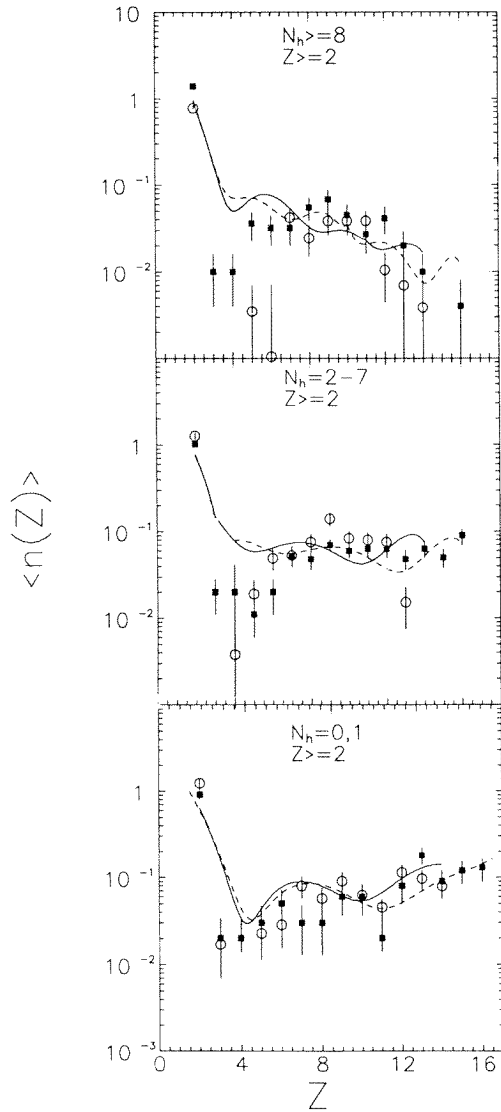


Figure 6. The charge distributions of projectile fragments in ^{28}Si (14.6 A GeV) and ^{32}S (3.7 A GeV) interactions: bottom, with a quasinucleon type; middle, with the CNO type and top, with AgBr type. The full and broken curves represent the corresponding calculations using the combined model for ^{28}Si and ^{32}S , respectively.

with fragments of large Z values. In other words, when the collision occurs with a heavy target nucleus (Br or Ag), the probability of producing heavy PFs decreases.

It can be also seen in figure 6 that all three panels seem to show a strong depression for $3 \leq Z \leq 5$ which is only mildly present in the calculations for $N_h = 0, 1$. Such a depression has not been seen for the fragmentation of heavier nuclei and seems to be a particular feature of these light alpha cluster nuclei. Similar findings were obtained by Adamovich *et al* [1] for these light alpha cluster nuclei. The combined model is able to describe this region only in the case of quasinucleon interactions.

Figure 7 shows the multiplicity distributions of the PFS with charges $Z \geq 2$ produced from the interactions with nuclear emulsion of ^{28}Si at (14.6 A GeV) and ^{32}S at (3.7 A GeV) as a function of N_h (i.e. at $N_h = 0, 1, 2 \leq N_h \leq 7$ and $N_h \geq 8$). The full and broken histograms represent the calculations according to the combined model for ^{28}Si and ^{32}S ,

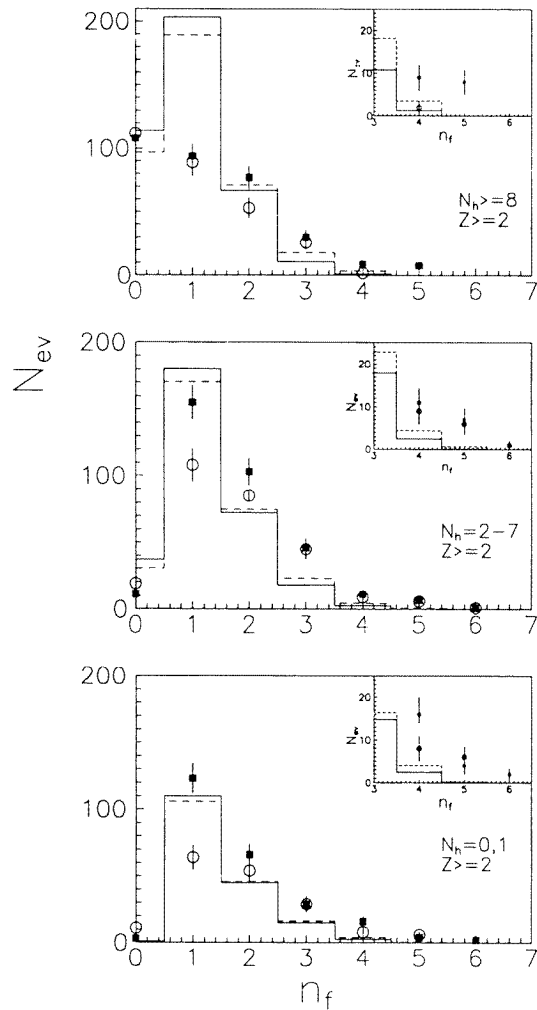


Figure 7. The multiplicity distributions of fragments with charge $Z \geq 2$ in ^{28}Si (14.6 A GeV) and ^{32}S (3.7 A GeV) interactions: bottom, with a quasinucleon type; middle, with the CNO type and top, with AgBr type. The notation is identical to that in figure 5. The inserts show the same distributions for $n_f < 6$.

respectively. The calculations are normalized to the experimental data. The results of the calculations indicate that the mean number of fragments increases with increasing target size.

Investigating the ratio between the experimental number of events in the case of ^{32}S and the corresponding number for ^{28}Si it can be noticed that:

- for the production of one fragment (i.e. $n_f = 1$), this ratio decreases as N_h increases such that it equals ~ 2 , ~ 1.5 and ~ 1 for the three N_h ranges, respectively i.e. this production is energy dependent in the first two ranges of N_h ;
- concerning the emission of two fragments, the ratio is somewhat greater than 1 for all N_h values;
- as for n_f values ≥ 3 , the ratio tends to be nearly equal to one over the three studied ranges of N_h .

It can also be noticed from figure 7 that the majority ($\sim 89\%$) of events with $n_f = 0$ (i.e. those where all the emanating PFS have $Z < 2$) occur in the $N_h \geq 8$ range.

On the whole, the combined model reasonably describes the main features of the data.

5. Concluding remarks

Experimental data on the fragmentation of ^{28}Si (at 14.6 A GeV) and ^{32}S (at 3.7 A GeV) in the interactions with different emulsion nuclei are presented and compared with a kind of hybrid model. The results obtained from this study lead to the following conclusions.

(1) The experimental cross section of total projectile disintegration events are reproduced by the Glauber approach, using Reggeon parametrization of the NN scattering amplitude.

(2) The estimation method of charge and excitation energy of the projectile residues created in the interaction with various targets of the emulsion nuclei allows the explanation of the Q value of the reaction.

(3) The charge, size and multiplicity distributions of PFS are nearly beam-energy independent. Thus, the limiting fragmentation hypothesis is verified for the process of ^{28}Si (at 14.6 A GeV) and ^{32}S (at 3.7 A GeV) fragmentation. This suggests that the beam energy is of little importance for the nuclear fragmentation process except possibly for the most peripheral interactions.

(4) The charge and multiplicity distributions of fragments are described by assuming that the spectator parts either decay by slow evaporation or fast multifragmentation (according to the phenomenological evaporation-percolation approach). For quasinucleon events, where the size of the fragmenting system is experimentally well defined, the charge distribution can be predicted by the combined model. While for the interactions with CNO and AgBr types, the description is good except in the region $3 \leq Z \leq 5$.

(5) The multiplicity distribution for PFS having $Z \geq 3$ in ^{28}Si and ^{32}S ions are similar for all ranges of N_h .

(6) In central and near-central events the probability of producing heavy PFS decreases, while for quasinucleon target events ($N_h = 0, 1$) there is an enhancement of heavy fragments.

Acknowledgments

The authors are grateful to Professor P L Jain of the State University of New York for supplying emulsion plates of Si (14.6 A GeV). They are also grateful to Professor A M Baldwin and Professor A D Kovalenko from JINR, Dubna for their help in the exposure of S (3.7 A GeV) emulsion stacks.

References

- [1] Adamovich M I *et al* (EMU01 collaboration) 1995 *Z. Phys. A* **351** 311
- [2] Lynen U *et al* 1992 *Nucl. Phys. A* **545** 329
Jain P L, Singh G and El-Nagdy M S 1992 *Phys. Rev. Lett.* **68** 1656
- [3] Schuettauf *et al* 1996 *Nucl. Phys. A* **607** 457
- [4] Hsi W-C *et al* 1997 *Phys. Rev. Lett.* **79** 817
- [5] Kiselev S M 1994 *Nucl. Phys. A* **579** 643
Aichelin J 1991 *Phys. Rep.* **202** 233
- [6] Andersson B *et al* 1987 *Nucl. Phys. B* **281** 289
Nilsson-Almqvist B and Stenlund E 1987 *Comput. Phys. Commun.* **43** 387
- [7] Werner K 1993 *Phys. Rep.* **232** 87
- [8] Capella A, Sukhatme U, Tan C I and Tran Thanh Van J 1994 *Phys. Rep.* **236** 227
- [9] Bondorf J B *et al* 1995 *Phys. Rep.* **257** 134
- [10] Gross D H E 1990 *Rep. Prog. Phys.* **53** 605
- [11] Maruyama T and Nitta K 1995 *Phys. Lett. B* **385** 34
- [12] Abdel-Waged Kh and Uzhinskii V V 1997 *Phys. Atom. Nuclei* **60** 828

- [13] El-Nadi M, Abdel-Salam A, Hussein A, Shaat E A, Ali-Mousa N, Abou-Mousa Z, Kamel S, Abdel-Waged Kh and El-Falaky E 1997 *Int. J. Mod. Phys. E* **6** 191
- [14] Abdel-Waged Kh and Uzhinskii V V 1998 *J. Phys. G: Nucl. Part. Phys.* **24** 1723
- [15] Adamovich M I et al (EMU01 collaboration) 1997 *Z. Phys. A* **358** 337
- [16] El-Nadi M, Abdel-Salam A, Hussien A, Shaat E, Ali-Mousa N, Abou-Mousa Z and El-Falaky E 1995 *Nuovo Cimento A* **108** 831
- [17] Singh G, Ismail A Z M and Jain P L 1991 *Phys. Rev. C* **43** 2417
- [18] Ismail A Z M, El-Nagdy M S, Gomber K L, Aggarwal M M and Jain P L 1984 *Phys. Rev. Lett.* **52** 1280
- [19] Singh G, Jain P L and El-Nagdy M S 1992 *Europhys. Lett. A* **7** 113 and references therein
El-Nadi M et al to be published
- [20] Aurenche P et al 1992 *Phys. Rev. D* **45** 92
- [21] Shmakov S Yu, Uzhinskii V V and Zadarozhny A M 1989 *Comput. Phys. Commun.* **54** 125
- [22] Galperin A S and Uzhinskii V V 1994 *JINR E2-94-505*
- [23] Abramovskii V A et al 1973 *Sov. J. Nucl. Phys.* **18** 308
- [24] Borekov K G et al 1991 *Sov. J. Nucl. Phys.* **53** 569
- [25] Stenlund E and Otterlund I 1982 *Nucl. Phys. B* **198** 407
- [26] Campi X, Desbois J and Liparini E 1984 *Nucl. Phys. A* **428** 327c
- [27] Weisskopf V 1937 *Phys. Rev.* **52** 295
Friedman W A 1983 *Phys. Rev. C* **28** 16
- [28] Pan J and Das Gupta S 1995 *Phys. Rev. C* **51** 1384
- [29] Abul-Magd A Y, Friedman W A and Hufner J 1986 *Phys. Rev. C* **34** 113
- [30] Cole A J and Cherkaoui-Tadili R 1987 *Phys. Rev. C* **36** 1484
- [31] El-Nadi M, Abdel-Salam A, Hussien A, Shaat E A, Ali-Moussa N, Abou Moussa Z, Kamel S, Abdel-Waged Kh, El-Falaky E and Fayed M 1997 *Radiat. Measure.* **28** 231